



INJECTABLE BONE CEMENT BASED ON CALCIUM SILICATE AND CALCIUM PHOSPHATE

NASSER Y. MOSTAFA^{a*} and Z. I. ZAKI^b

Chemistry Department, Faculty of Science, Taif University, 888 Hawayia, TAIF, SAUDI ARABIA

^aChemistry Department, Faculty of Science, Suez Canal University, ISMAILIA 41522, EGYPT

^bAdvanced Materials Division, Central Metallurgical R&D Institute (CMRDI),

P.O. Box: 87 Helwan, CAIRO, EGYPT

ABSTRACT

The development of injectable bone cement has been recognized as a promising strategy to fulfill the complex requirements of biomaterials for micro-invasive surgeries. The purpose of this study was to develop a novel injectable bioactive bone cement based on tricalcium silicate (TCS)- α -tricalcium phosphate (α -TCP) composites. Different bone cement formulations were prepared by varying the TCS contents (0, 3.2, 9.9 and 11.8% mole of TCS). The hydration experiments were carried out at 37°C. Injectabilities, setting times and mechanical properties of the final composites were determined. The results indicate that TCS delays the conversion of α -TCP into calcium-deficient hydroxyapatite (CDHAP). The produced CDHAP in the presence of TCS was modified by partial substitution silicate ion in place of phosphate. Also, $\text{Ca}(\text{OH})_2$ produced from TCS hydration inter CDHAP and increases the $\text{Ca}/(\text{P}+\text{Si})$ molar ratio.

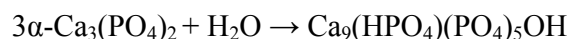
Key words: Tricalcium phosphate, Bone cement, Tricalcium silicate, Physico-mechanical properties, Injectability.

INTRODUCTION

Minimally invasive technique is a newly emerging surgical technique^{1,2}, which includes micro-invasive bone grafting. Micro-invasive bone grafting means that the bone is taken out and bone graft materials are delivered to the desired site through a small incision or even local percutaneous puncture and injection³. So the grafts used in this procedure may be viscous suspension of fine particulate materials⁴. It has many advantages such as little injury, simple procedures and fast recovery. Limited sources of graft materials with suitable injectability and mechanical properties are the main factors affecting the development of the technique⁵. Therefore, to prepare a stable, economical, efficient and easy-to-use injectable graft material is crucial for the development of the technique.

* Author for correspondence; E-mail: nmost69@yahoo.com; Tel.: +20-64-382216; Fax: +20-64-322381

Calcium phosphate cements (CPC) are clinically valuable due to their biocompatibility, ease of handling, moldability, and ability to set or harden at body temperature⁶. Generally, they consist of a mixture of an aqueous solution and one or several calcium phosphate powders⁷. Many CPC formulations have been proposed, in particular those based on the use of α -tricalcium phosphate (α -Ca₃(PO₄)₂; α -TCP)⁸. Tricalcium phosphate exists in two crystalline forms; α -TCP and β -TCP, whereas β -TCP is the low temperature stable form. Thus, preparation of α -TCP form involves rapid cooling from high temperatures (> 1200°C) to room temperature. The hydrolysis of α -TCP involves the dissolution of α -TCP and the formation of calcium-deficient hydroxyapatite (CDHAP) according to the following equation⁹⁻¹¹:



α -TCP powders used in CPCs are generally obtained by a combination of sintering and milling procedures⁹⁻¹⁴ and start reacting within seconds after contacting an aqueous solution^{12,13}. The drawbacks of CPC, including low strength and poor injectability¹⁴⁻²⁰, have limited its clinical use. To be used clinically, α -TCP reactivity has to be appropriately adjusted to control hardening and setting rate²¹. Ideally the cement should hardly react during mixing and application, and then rapidly harden. Some researchers used additives such as phosphate ions or hydroxyapatite (HAP) to control setting and hardening^{10,22}. Another approach is to prolong the milling duration of the raw materials to make them more reactive^{9,23,24}. Unfortunately, these approaches are not good enough for some applications such as injectable bone cement, for which the viscosity during application should be in a defined range, and hardening should then proceed fast²⁵. In a recent study²⁶, the injectability of the CPC paste was dramatically improved using hydroxypropyl methylcellulose.

Zhao et al.^{27,28} have shown that tricalcium silicate (Ca₃SiO₅; TCS) had good hydraulic properties and excellent bioactivity. However, there are many complications in using tricalcium silicate cement in clinical bone filling application. One of these complications is the long setting time of tricalcium silicate cement²⁷⁻²⁹. Another complication associated with the large amount of calcium hydroxide [Ca(OH)₂] formed during hydration reaction, which causes a high rise of the pH up to 12.²⁷ This could have an adverse impact on the biocompatibility. Recently, Sprio et al.³⁰ developed load-bearing bone composites, made of hydroxyapatite (HAP) and bioactive calcium silicate as a reinforcing phase.

The combination of combustion and a reactive solution approach leads to the so-called solution combustion synthesis (SCS) method³¹⁻³⁴. SCS synthesis using metal nitrates as oxidants and different organic compounds such as citric acid, α -alanine, glycine and urea are used as fuel, is a useful technique for synthesis of high purity nanomaterials³⁵⁻³⁸. Particle

size and powder morphology of the product can be optimized by varying the different process parameters during the synthesis.

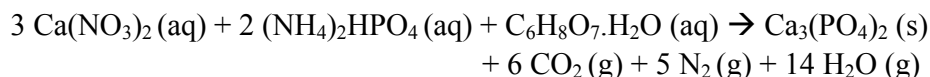
This work is aimed at developing novel fully synthetic injectable bone cement based on tricalcium silicate and tricalcium phosphate. The expected hydration products after injection and *in situ* setting, is nanohydroxyapatite with silicon substitution and with no or minimum amount of $\text{Ca}(\text{OH})_2$.

EXPERIMENTAL

Materials and methods

Combustion synthesis of α -TCP

α -TCP powders of nanoparticle size were synthesized using solution combustion synthesis (SCS). Calcium nitrate ($\text{Ca}(\text{NO}_3)_2 \cdot 4\text{H}_2\text{O}$) and dibasic ammonium phosphate $(\text{NH}_4)_2(\text{HPO}_4)$ were used as reactants and citric acid ($\text{C}_6\text{H}_8\text{O}_7 \cdot \text{H}_2\text{O}$) was used as a fuel. Combinations of both salt reactants and the fuels was tailored to give the reducing/oxidation power of unity³⁸. The formation of tricalcium phosphate by SCS assuming complete combustion can be represented by the following reaction:



Stoichiometric composition of the redox mixture was dissolved in the minimum amount of water. The white precipitate was dissolved using the minimum amount of nitric acid with stirring. The aqueous solution containing the redox mixture in a Pyrex container introduced in a muffle furnace preheated to 750°C , until undergoes flameless combustion. The ignition product was calcinated at 1400°C for 5 hrs. Rapid cooling of the products using chilled flat steel pan produces α -TCP as confirmed by XRD as shown in Fig. 1. The resultant powders were grounded and sieved to 300-mesh for further experiments.

Tricalcium silicate (TCS) preparation

Tricalcium silicate (TCS) was synthesized by conventional solid state route as previously stated³⁹. The stoichiometric mixture of pure grade calcium carbonate and 5 μm Min-U-Sil silica was ball milled in hexane with zirconia balls for 20 hrs. The mixture was heated at 1350°C for 5 hrs and air quenched. XRD analysis shows the sample to be completely converted to pure monoclinic TCS as shown in Fig. 2. The resultant powders were grounded and sieved to 300-mesh for further experiments.

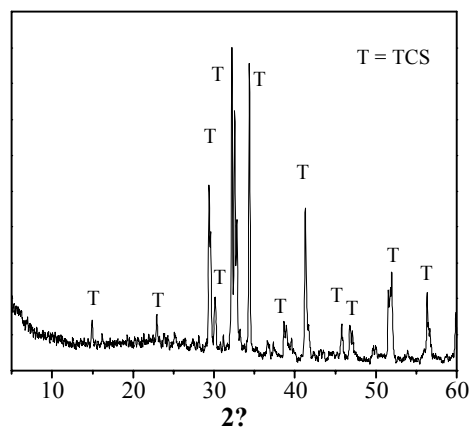


Fig. 1: XRD pattern of pure monoclinic TCS

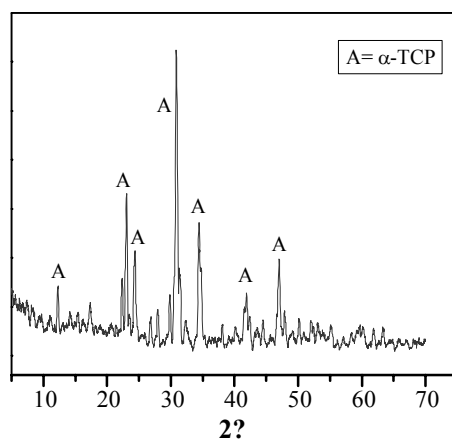


Fig. 2: XRD of α -TCP prepared by combustion synthesis method using citric acid as a fuel

Bone cement formulations

The relative proportion of α -TCP and TCS in each mix was selected according to Table 1. Mix TCPS0.33 expected to give near stoichiometric hydroxyapatite with silicon substitution [$\text{Ca}/(\text{P}+\text{Si}) = 1.67$] and no free $\text{Ca}(\text{OH})_2$. Assuming that, the produced $\text{Ca}(\text{OH})_2$ rapidly reacts with CDHAP to produce hydroxyapatite and silicate ions substituted in HAP crystal structure. The α -TCP-TCS pre-composites were prepared by mixing the solid powders in absolute ethanol, then ethanol was evaporated under vacuum. Pastes were prepared by mixing the pre-composites with deionized water at liquid to powder ratio (L/P ratio) of 0.60. After mixing for 2 min, the pastes were moved into Teflon molds (10 mm diameter 18 mm

high and 6 mm diameter 2 mm high) and stored at 37°C and 100% relative humidity (RH) for 7 days.

Table 1: Composition of injectable bone cements

Mix	α -TCP [Ca ₃ (PO ₄) ₂]	TCS [Ca ₃ SiO ₅]	% TCS (mole)	% TCS (weight)
TCP	3	0.0	0.0	0.0
TCPS0.10	3	0.1	3.2	2.4
TCPS0.33	3	0.33	9.9	7.6
TCPS0.40	3	0.4	11.8	8.9
TCS	-	1	100	100

Injectability and setting times

The injectability of the cements was tested by a 5 mL syringe, which was fitted with a needle of 1.6 mm inner diameter. After mixing the mixture of cement with liquid for two minutes, the as-prepared paste was poured into the syringe. Then a 5 Kg compressive load was mounted vertically on the top of the plunger for 2 min. The mass of the paste before and after injecting was measured. Each test was repeated for 3 times and the average value was calculated. The injectability was calculated according to the following equation:

$$\text{Injectability (\%)} = [\text{Paste wt. expelled form the syringe} / \text{Total paste wt.}] \times 100$$

The initial (IS) and the final (FS) setting times were measured with the Vicat needle according to ISO9597-1989E. The initial setting time is defined as the time necessary so that the light needle (280 g, 1.13 mm) plunges into the paste and has a span of 5 ± 1 mm to the tube bottom. The final setting time is defined as the time necessary so that the heavy needle (350 g, 2.0 mm) no longer leaves a visible print on the surface of the paste.

Characterization of the composites

After the composites were set for 7 days, they were transferred into acetone (100%) to stop hydration and vacuum-dried. X-ray diffraction (XRD) analysis was performed using an automated diffractometer (Philips type: PW1840), at a step size of 0.02° , scanning rate of 2° in $2\theta/\text{min}$, and a 2θ range from 4° to 80° . All samples were coated with gold. FTIR

spectroscopic measurements were carried out using a spectrometer (FTIR, JASCO 470). The samples were mixed with KBr with a sample/KBr weight ratio of 1/100 and compressed to give self-supporting pellets. The compressive strength was measured on the samples with diameter of 10 mm and height of 18 mm at a loading rate of 0.5 mm min⁻¹ using a universal testing machine (Instron-1195). Three replicates were carried out for each sample.

***In vitro* degradation of cement pastes**

The 7-day-set paste disks were soaked in phosphate buffered (pH = 7.3-7.4) at 37°C in shaking water bath for 1, 3, 7 and 28 days with cement paste/buffer ratio of 1.50 mg/mL. The solution was refreshed every 2 days. After the set soaking time, the disks were dried under vacuum for 24 hr and the final weight of each sample was measured accurately. The degradation rate was calculated as the percent weight loss. The weight loss (WL) was calculated as follows:

$$WL \% = [(W_i - W) / W_i] \times 100$$

Where, W_i is the initial weight of the specimen and W is the weight of the specimen dried after different degradation time. Each measurement was performed three times and the average value was calculated.

RESULTS AND DISCUSSION

Setting times and injectability

Experiments were performed to evaluate the influence of TCS contents on α -TCP cement setting, at L/P ratio of 0.60. The results in Table 2 indicated that the TCS contents greatly affected both the initial setting (IS) and the final setting (FS) times. Pure TCP paste has initial (IS) and final (FS) setting time of 38 min and 77 min, respectively. An increase in setting times were observed with the increase of the TCS contents. Increasing TCS content to 11.8% mole (mix TCPS0.4) resulted in an increase in initial setting (IS) from 38 to 85 min and final setting (FS) from 77 to 124 min, respectively. The hydration of TCS produce amorphous CSH-gel, which cover the unhydrated TCP grains and delay the hydration reaction. Pure TCS paste has initial (I) and final (F) setting time of 115 min and 195 min, respectively.

The effect of TCS contents on the injectability of the α -TCP pastes, prepared at L/P = 0.60, is given in Table 2. Increasing the TCS contents significantly improved the paste

injectability. Generally, cement injectability increased with increasing the TCS contents. The injectability of the paste without TCS (mix TCP) was 85%, and it increased to 100% at a TCS contents of 11.8% mole (mix TCPS0.4). Pure TCS paste could be nearly completely extruded (100% injectable), as shown in Table 1. This can be explained by the fact that the setting time of TCS is longer than that of TCP.

Table 2: Initial setting (IS) time, final setting (FS) time and injectability of the α -TCP paste with various amounts of TCS

Mix	TCP	TCPS0.1	TCPS0.33	TCPS0.4	TCS
IS (min.)	38	45	63	85	115
FS (min.)	77	85	94	124	195
Injectability (%)	82	90	96	100	100

Compressive strength

Figure 3 shows the compressive strength of different pastes after setting for 7 days in a 100% humidity water bath at 37°C. The result indicated that the compressive strength of TCP + TCS composite pastes were lower than that of pure TCP paste and much lower than of that of pure TCS paste. Among the TCP + TCS composite pastes with different TCS contents, the one with 11.8 % mole (TCPS0.4) had the highest compressive strength, which was slightly lower than that of pure TCP paste (mix TCP).

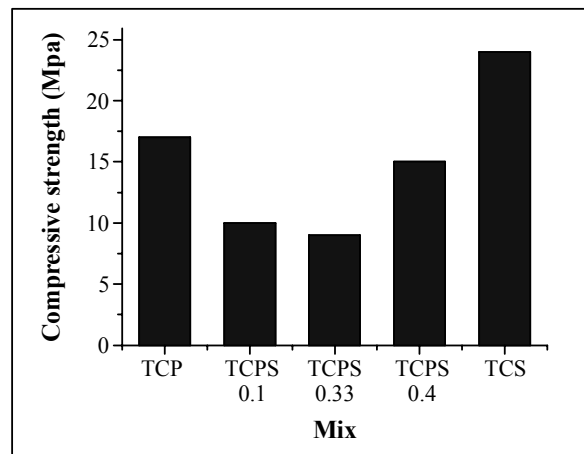
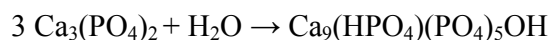


Fig. 3: The compressive strength of the cement pastes with different TCS contents after 7 days at 37 °C and 100% humidity

XRD analysis

Fig. 4, shows the XRD patterns of TCP, TCS and TCPS0.33 pastes hydrated for 7 days at 37°C and 100% relative humidity. In TCP paste, all the identified peaks were corresponding to calcium deficient hydroxyapatite (CDHAP) and the intensity of α -TCP peaks were almost negligible (Fig. 4 (a)). When the α -TCP powder is mixed with water, α -TCP hydrolyses to CDHAP according to the equation⁹⁻¹¹:

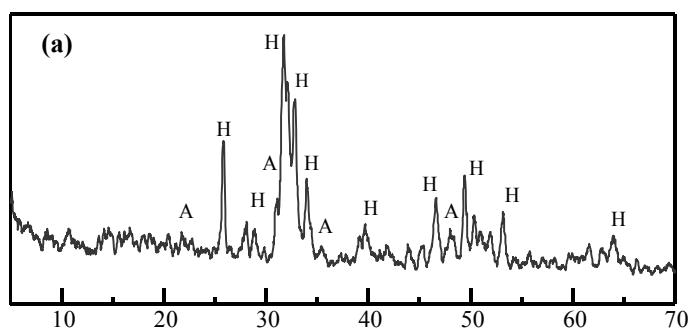


This transformation is responsible for the hardening of the cement paste.

Fig. 4 (b), shows the XRD pattern of TCS paste hydrated for 7 days. There was a remarkable change in XRD pattern of TCS paste than that of the unhydrated TCS powder (Fig. 2). A new broad peak centered at $2\theta = 29.04^\circ$ appeared due to the formation of semicrystalline calcium silicate hydrate gel (CSH), and the intensity of TCS peaks was almost negligible. In addition, calcium hydroxide appeared due to the hydration of TCS³⁹ according to the following equation:



The XRD spectra of the α -TCP cements containing 9.9% mole TCS (mix TCPS0.33) is illustrated in Fig. 4 (c). The XRD spectra indicated that the addition of TCS up to mix TCPS0.33 did not change the hydration reaction of α -TCP and that the reaction product were mainly silicon substituted hydroxyapatite and no free $\text{Ca}(\text{OH})_2$ peaks was observed. The peaks of unreacted α -TCP are higher than those present in TCP mix (Fig. 4 (a)). This clearly demonstrate that TCS retards the hydration of α -TCP.



Cont...

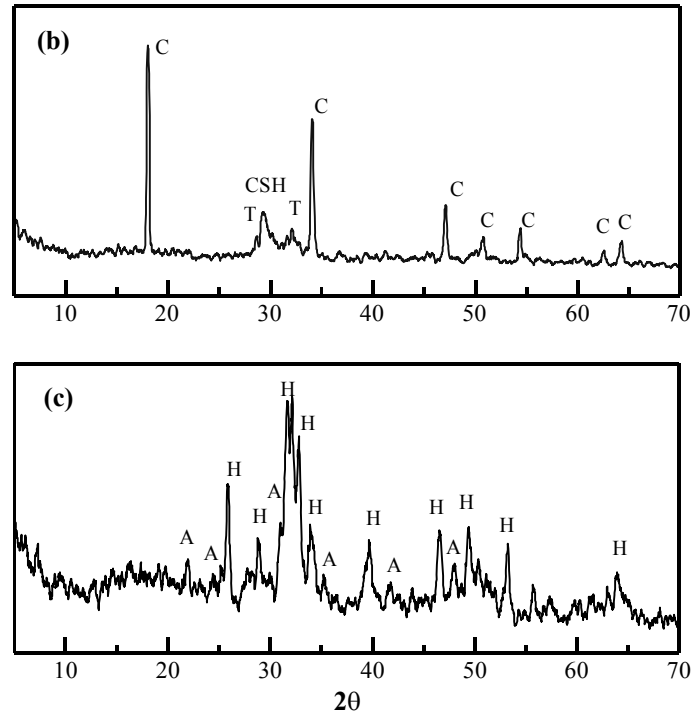


Fig. 4: XRD of cement pastes hydrated for 7 days at 37°C; (a) TCP, (b) TCPS0.33 and (c) TCS (H= hydroxyapatite, A= α -TCP, T=TCS, CSH = calcium silicate hydrate and C= $\text{Ca}(\text{OH})_2$)

FTIR spectra

The vibrational spectra of different cement pastes hydrated for 7 days at 37°C are shown in Fig. 5. The vibrational spectra of all samples can be divided into three groups of bands. The first group is due to stretching and bending vibrations of water molecules and O-H groups. The second group is due to CO_3^{2-} vibration. The third group is those due to the phosphate and silicate tetrahedra vibrations. Since the vibrations in these groups are not usually coupled to each other, we shall discuss them separately.

Water molecules and hydroxyl bands

All the spectra have a broad band at $3400\text{--}3200\text{ cm}^{-1}$, due to stretching vibrations of O-H groups of adsorbed H_2O . This broadening is because of the formation of hydrogen bonding with a wide range of strengths^{40,41}. It is well known that as hydrogen bonding strength increases, the stretching vibrations frequency of O-H group decreases⁴². The bending vibration band of molecular H_2O appears at 1641 cm^{-1} .

The bands correspond to stretching and bending modes of the hydroxyl groups in hexagonal channels of hydroxyapatite structure appears at 3571 and 631 cm^{-1} , respectively⁴⁰. Fig. 5, shows that these bands appear as shoulders in samples TCP and TCPS0.1. However, they completely disappears in sample TCPS0.33. This is in agreement with our previous results⁴⁰. These bands decrease with increasing silicate substitution level and both bands nearly disappear at certain substitution level. Many investigators^{40,43,44} have accounted for the decrease of O-H bands by the charge compensation mechanism in which HAP unit cell loses one OH^- group for the substitution of the phosphate group by silicate group. The stretching mode of O-H in $\text{Ca}(\text{OH})_2$ gives rise to a sharp signal at 3644 cm^{-1} ⁴⁵ in samples TCS and TCPS0.4.

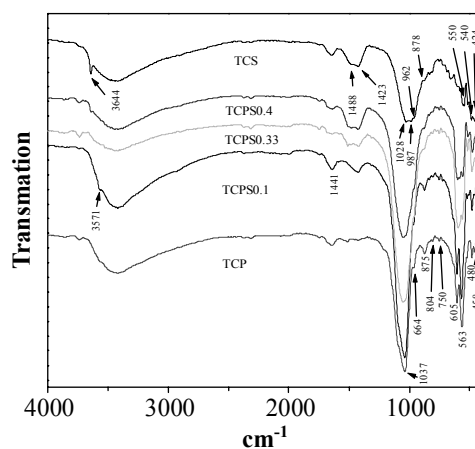


Fig. 5: FTIR spectra of hydration products of different mixes of α -TCP + TCS mixes at 7 days

Carbonate bands

Although no carbonates are detected by XRD analysis, CO_3^{2-} bands appears in the FTIR spectra of all samples. This is due to contamination with CO_2 during samples preparations and drying. The samples contains $\text{Ca}(\text{OH})_2$ have high amounts of carbonate, because $\text{Ca}(\text{OH})_2$ reacts with CO_2 gas. The carbonate bands appear in all hydroxyapatite samples at 1486 – 1418 cm^{-1} and 875 cm^{-1} . These correspond to the CO_3^{2-} groups substitute for phosphate groups in the apatite. This substitution is named a B-type, similar to biological carbonate-HAP⁴⁶.

In TCS and TCPS0.4 pastes, the partially resolved doublet peak at 1423 and 1487 cm^{-1} is attributed to carbonate species for the reaction of atmospheric CO_2 with $\text{Ca}(\text{OH})_2$. The weak band at ~ 878 cm^{-1} , in TCS and TCPS0.4, is due to the out-of-plane bending of CO_3^{2-} .

Phosphate and silicate bands

The strong bands in the range 900-1200 cm^{-1} correspond to P-O stretching vibration modes of the phosphate groups. The doublet at 605-563 cm^{-1} corresponds to the O-P-O bending mode. The infrared P-O stretching bands and O-P-O bending bands decrease and become less resolved as the silicate contents increase, as shown in Fig. 5. However, the positions of both stretching and bending bands are obviously unaffected by the silicate substitution.

In TCS paste the asymmetrical stretching vibrations of SiO_4 tetrahedra appear as a complex group of bands in the range of 900-1100 cm^{-1} . The second most intense silicate bands are broadly characterized as O-Si-O deformation or bending modes, which occur in the 556-400 cm^{-1} region and the band at $\sim 687 \text{ cm}^{-1}$ is due to Si-O-Si bending vibrations. Yu et al.⁴⁷ was able to assign different stretching bands of Si-O in calcium silicate hydrates by comparing results from ^{29}Si MAS NMR and FTIR for the same set of samples. They assigned band at 811 cm^{-1} to Si-O stretching of Q^1 sites (end chain silicate tetrahedra). Bands corresponding to Si-O stretching of Q^2 sites appears at 987 cm^{-1} and 1028 cm^{-1} . Yu et al.⁴⁷ were able to assign band at 811 cm^{-1} to Si-O stretching of dimer silicate chains. This band appears very weak in mix TCPS0.4, which indicates the start of calcium silicate hydrate (CSH) formation.

Fig. 5, clearly shows that, in sample TCPS0.4, the stretching vibration bands of silicate interfere with phosphate stretching vibration bands that result in the observed broadening of the latter.

In vitro degradation of cement pastes

The 7-day hydrated cement pastes were soaked in phosphate buffered (pH = 7.3-7.4) at 37°C in shaking water bath for 1, 3, 7 and 28 days. Table 3 shows the weight loss (wt. %) at versus soaking time for the cements with different TCS contents. The weight loss of the cement pastes were declined as the TCS contents increase in the initial cement mix. It was clear to see that, with the addition of TCS, the degradation rate of the composite paste was significantly lower than that of pure TCP paste and the degradation rate of the composite decreased with the increase of TCS contents.

The self-setting properties, such as injectability and setting times, are the most important factors that control the applicability of self-setting injectable cement. In this paper, composite cements were designed and prepared by mixing the α -TCP with tricalcium silicate. The setting time, injectability, mechanical properties and *in vitro* degradation in phosphate buffer were evaluated and compared with those of the pure α -TCP and pure TCS cements.

Table 3: Weight loss (wt. %) at different soaking time for cements with different TCS contents

Sample	TCP	TCPS0.1	TCPS0.33	TCPS0.4	TCS
1 day	20.2	18.8	17.2	16.5	1.1
3 days	22.8	19.1	17.6	17.1	1.2
7 days	25.3	21.4	17.8	17.6	2.1
28 days	25.8	22.5	18.3	18.1	9.6

The self-setting property of TCS paste is due to the progressive dissolution of Ca^{2+} and SiO_4^{4-} ions from TCS and the deposition of a nanoporous, semicrystalline CSH gel. The amorphous CSH gel is deposited on the original Ca_3SiO_5 , while $\text{Ca}(\text{OH})_2$ crystals nucleate and grow in the available capillary pore space in pure TCS paste. As time proceeds, the CSH gels polymerize and harden. This phenomenon suggests that the self-setting progress is mainly attributed to the formation of a solid network, which is also associated with the densification and increase of the mechanical strength.

In pastes contain TCP and TCS, the hydration of TCS produces amorphous CSH gel that deposited on α -TCP surface and delays its hydration reaction. Meanwhile, calcium hydroxide produced from TCS hydration reacts with CDHAP to change it to close to the stoichiometric HAP. The compressive strength of the α -TCP cement pastes decreases with increasing TCS contents. Whereas the compressive strength of the pure TCS paste reached 23 MPa after 7 days hydration time.

As the TCS contents increased, the spectra did not alter except the appearance of $\text{Ca}(\text{OH})_2$ was clearly detected when the TCS content increased to 11.8% mole (mix TCPS0.4).

CONCLUSION

In this investigation, novel bioactive composite cements were prepared by mixing tricalcium silicate with α -TCP. The α -TCP/TCS composite cements showed a longer setting times and improved injectability. However, the mechanical strength decreased with TCS addition up to 11.0% compared with both pure TCP and pure TCS cements.

In the present investigation, addition of TCS to α -TCP bone cements improve the injectability of the cement pastes and increases setting time. The combined hydration of the

TCP and TCS yielded a bioactive silicon-substituted HAP. Furthermore, the released Ca(OH)_2 reacts with CDHAP to drive it to more stoichiometry.

The addition of TCS to α -TCP cement system had deaccelerating effect on the precipitation of CDHAP crystals. Moreover, it improved injectability without damaging significantly its mechanical properties. Combining, injectability, self-setting and expected superior bioactivity of the produced silicon-substituted hydroxyapatite in a single bone cement material represents a step forward in the design of new materials for bone regeneration compatible with minimally invasive surgical techniques. However, further *in vivo* studies are required to confirm the possible application.

ACKNOWLEDGEMENT

This work was financially supported by a grant from Taif University (Grant No. 1-434-2485).

REFERENCES

1. L. M. Brunt, Minimal Access Adrenal Surgery, *Surg Endosc*, **20**, 351-61 (2006).
2. N. Marotta, M. Cosar, L. Pimenta and L. T. Khoo, A Novel Minimally Invasive Presacral Approach and Instrumentation Technique for Anterior L5-S1 Intervertebral Discectomy and Fusion: Technical Description and Case Presentations, *Neurosurg Focus*, **20**, E9 (2006).
3. J. Maneerit, S. Meknavin and S. Hanpanitkitkan, Percutaneous Versus Open Bone Grafting in the Treatment of Tibial Fractures: A Randomized Prospective Trial, *J. Med. Assoc. Thai.*, **87**, 1034-1040 (2004).
4. H. Liu, H. Li, W. Cheng, Y. Yang, M. Zhu and C. Zhou, Novel Injectable Calcium Hydroxide/Chitosan Composites for Bone Substitute Materials, *Acta Biomater*, **2**, 557-565 (2006).
5. M. C. Kruyt, C. Persson, G. Johansson, W. J. Dhert and J. D. de Bruijn, Towards Injectable Cell-Based Tissue-Engineered Bone: The Effect of Different Calcium Phosphate Microparticles and Pre-culturing. *Tissue Eng.*, **12**, 309-317 (2006).
6. P. K. Bajpai, C. M. Fuchs and D. E. McCullum, Development of Tricalcium Phosphate Ceramic Cements, in, J. E. Lemons, Editor, *Quantitative Characterization and Performance of Porous Implants for Hard Tissue Applications*, ASTM, Philadelphia, PA (1987) pp. 377-388.

7. W. E. Brown and L. C. Chow, A New Calcium Phosphate Setting Cement, *J. Dent. Res.*, **62**, 672 (1983).
8. M. Bohner, U. Gbureck and J. E. Barralet, Technological Issues for the Development of More Efficient Calcium Phosphate Bone Cements: A Critical Assessment, *Biomaterials*, **26(33)**, 6423-6429 (2005).
9. H. Monma and M. Goto, Behavior of the α - β Phase Transformation in Tricalcium Phosphate, *Yogyo-Kyokai-Shi*, **91(10)**, 473-475 (1983).
10. C. L. Camire, U. Gbureck, W. Hirsiger and M. Bohner, Correlating Crystallinity and Reactivity in an Alpha-Tricalcium Phosphate, *Biomaterials*, **26(16)** 2787-2794 (2005).
11. C. Durucan and P. W. Brown, Reactivity of Alpha-Tricalcium Phosphate, *J. Mater. Sci.*, **37(5)**, 963-969 (1999).
12. M. P. Ginebra, F. C. M. Driessens and J. A. Planell, Effect of the Particle Size on the Micro and Nanostructural Features of a Calcium Phosphate Cement: A Kinetic Analysis, *Biomaterials*, **25(17)**, 3453-3462 (2004).
13. M. Bohner, A. K. Malsy, C. L. Camire and U. Gbureck, Combining Particle Size Distribution and Isothermal Calorimetry Data to Determine the Reaction Kinetics of α -Tricalcium Phosphate–Water Mixtures, *Acta Biomater.*, **2(3)**, 343-348 (2006).
14. K. Ishikawa, Effects of Spherical Tetracalcium Phosphate on Injectability and Basic Properties of Apatitic Cement, *Key Eng. Mater.*, 240-242, 369-372 (2003).
15. I. Khairoun, M. G. Boltong, F. C. M. Driessens and J. A. Planell, Some Factors Controlling the Injectability of Calcium Phosphate Bone Cements, *J. Mater. Sci. Mater. in Med.*, **9**, 425-428 (1998).
16. M. P. Ginebra, A. Rilliard, E. Fernández, C. Elvira, J. S. Román and J. A. Planell, Mechanical and Rheological Improvement of a Calcium Phosphate Cement by the Addition of a Polymeric Drug, *J. Biomed. Mater. Res.*, **57**, 113-118 (2001).
17. S. Sarda, E. Fernández, M. Nilsson, M. Balcells and J. A. Planell, Kinetic Study of Citric Acid Influence on Calcium Phosphate Bone Cement as Water-Reducing Agent, *J. Biomed. Mater. Res.*, **61**, 653-659 (2002).
18. E. M. Ooms, E. A. Egglezos, J. G. C. Wolke and J. A. Jansen, Soft-Tissue Response to Injectable Calcium Phosphate Cements, *Biomaterials*, **24**, 749-757 (2003).
19. U. Gbureck, J. E. Barralet, K. Spatz, L. M. Grover and R. Thull, Ionic Modification of Calcium Phosphate Cement Viscosity: Part I: Hypodermic Injection and Strength Improvement of Apatite Cement, *Biomaterials*, **25**, 2187-2195 (2004).

20. M. Bohner and G. Baroud, Injectability of Calcium Phosphate Pastes, *Biomaterials*, **26**, 1553-1563 (2005).
21. M. Bohner, Reactivity of Calcium Phosphate Cements, *J. Mater. Chem.*, **17**, 3980-3986 (2007).
22. U. Gbureck, J. E. Barralet, L. Radu, H. G. Klinger and R. Thull, Amorphous Alpha-Tricalcium Phosphate: Preparation and Aqueous Setting Reaction, *J. Am. Ceram. Soc.*, **87(6)**, 1126-1132 (2004).
23. U. Gbureck, O. Grolms, J. E. Barralet, L. M. Grover and R. Thull, Mechanical Activation and Cement Formation of Beta-Tricalcium Phosphate, *Biomaterials*, **24(23)**, 4123-4131 (2003).
24. G. Baroud, M. Bohner, P. Heini and T. Steffen, Injection Biomechanics of Bone Cements used in Vertebroplasty, *Biomed. Mater. Eng.*, **14(4)**, 487-504 (2004).
25. M. Bohner, T. J. Brunner, N. Doebelin, R. Tang and W. J. Stark, Effect of Thermal Treatments on the Reactivity of Nanosized Tricalcium Phosphate Powders, *J. Mater. Chem.*, **18**, 4460-4467 (2008).
26. E. F. Burguera, H. H. K. Xu and M. D. Weir, Injectable and Rapid-Setting Calcium Phosphate Bone Cement with Dicalcium Phosphate Dihydrate, *J. Biomed. Mater. Res. B Appl. Biomater.*, **77(1)**, 126-134 (2006).
27. W. Y. Zhao and J. Chang, Sol-Gel Synthesis and *In Vitro* Bioactivity of Tricalcium Silicate Powders, *Mater. Lett.*, **58**, 2350-2353 (2004).
28. W. Y. Zhao, J. Y. Wang, W. Y. Zhai, Z. Wang and J. Chang, The Selfsetting Properties and *In Vitro* Bioactivity of Tricalcium Silicate, *Biomaterials*, **26**, 6113-6121 (2005).
29. J. S. Schweitzer, R. A. Livingston, C. Rolfs, H. W. Becker and S. Kubsy, Ion Beam Analysis of the Hydration of Tricalcium Silicate, *Nucl. Instrum. Methods B*, **207**, 80-84 (2003).
30. S. Sprio, A. Tampieri, G. Celotti and E. Landi, Development of Hydroxyapatite/ Calcium Silicate Composites Addressed to the Design of Load-Bearing Bone Scaffolds, *J. Mechanical Behavior of Biomed. Mater.*, **2(2)**, 147-155 (2009).
31. A. S. Mukasyan, C. Costello, K. Sherlock, D. Lafarga and A. Varma, Perovskite Membranes by Aqueous Combustion Synthesis: Synthesis and Properties, *Separ. Purif. Tech.*, **25**, 117 (2001).

32. K. Patil, S. Aruna and T. Mimani, Combustion Synthesis: An Update, *Curr. Opin. Sol. State Mater. Sci.*, **6**, 507-512 (2003).
33. A. Varma, A. S. Mukasyan, K. Deshpande, P. Pranda and P. Erii, Combustion Synthesis of Nanoscale Oxide Powders: Mechanism, Characterization and Properties, *Mat. Res. Soc. Symp. Proc.*, **800**, 113-121 (2003).
34. K. Deshpande, A. S. Mukasyan and A. Varma, Direct Synthesis of Iron Oxide Nanopowders by Combustion Approach: Reaction Mechanism and Properties, *Chem. Mater.*, **16(24)**, 4896-4904 (2004).
35. M. V. Kuznetsov, I. P. Parkin, D. J. Caruana and Y. G. Morozov, Combustion Synthesis of Alkaline-earth Substituted Lanthanum Manganites; LaMnO_3 , $\text{La}_{0.6}\text{Ca}_{0.4}\text{MnO}_3$ and $\text{La}_{0.6}\text{Sr}_{0.4}\text{MnO}_3$, *J. Mater. Chem.*, **14**, 1377-1382 (2004).
36. K. Deshpande, A. S. Mukasyan and A. Varma, Aqueous Combustion Synthesis of Strontium-Doped Lanthanum Chromite Ceramics, *J. Am. Ceram. Soc.*, **86**, 1149-1154 (2003).
37. S. Deka and P. A. Joy, Characterization of Nanosized NiZn Ferrite Powders Synthesized by an Autocombustion Method, *Materials Chemistry and Physics*, **100**, 98-101 (2006).
38. K. C. Patil, M. S. Hegde, Tanu Rattan and S. T. Aruna, *Chemistry of Nanocrystalline Oxide Materials: Combustion Synthesis, Properties and Applications*, World Scientific Publishing Co. Pt. Ltd., Singapore (2008).
39. N. Y. Mostafa, H. Omar and S. A. Abo-El-Enein, Sulfate Attack on Pure Calcium Silicate Hydrates Phases, *Silicate Industrials*, **73(7-8)**, 117-123 (2008).
40. N. Y. Mostafa, H. M. Hassan and O. H. Abd Elkader, Preparation and Characterization of Na^+ , SiO_4^{4-} and CO_3^{2-} Co-Substituted Hydroxyapatite, *J. American Ceramic Society*, DOI: 10.1111/j.1551-2916.2010.04282.x (2010).
41. N. Y. Mostafa, E. A. Kishar and S. A. Abo-El-Enein, FTIR Study and Cation Exchange Capacity of Fe^{3+} - and Mg^{2+} -Substituted Calcium Silicate Hydrates, *J. Alloys and Compounds*, **473(1-2)**, 538-542 (2009).
42. P. F. McMillan, *Volatiles in Magmas*, *Reviews in Mineralogy*, Edited by M. R. Carroll and J. R. Holloway, Mineralogical Society of America, Washington, D.C., **30**, 131-155 (1994).
43. M. Palard, E. Champion and S. Foucaud, Synthesis of Silicated Hydroxyapatite $\text{Ca}_{10}(\text{PO}_4)_{6-x}(\text{SiO}_4)_x(\text{OH})_{2-x}$, *J. Solid State Chem.*, **181**, 1950-1960 (2008).

44. T. X. Lian, X. X. Feng and L. R. Fang, Structural Characterization of Silicon-Substituted Hydroxyapatite Synthesized by a Hydrothermal Method, *Mater. Lett.*, **59**, 3841-3846 (2005).
45. N. J. Coleman, K. Awosanya and J. W. Nicholson, Aspects of the *In Vitro* Bioactivity of Hydraulic Calcium (Alumino) Silicate Cement, *J. Biom. Mater. Res.*, **90A (1)**, 166-174 (2008).
46. J. A. Stephen, C. Pace, J. M. S. Skakle and I. R. Gibson, Comparison of Carbonate Hydroxyapatite with and without Sodium Co-Substitution, *Key Engineering Materials*, 330-332, 19-22 (2007).
47. P. Yu, R. J. Kirkpatrick, B. Poe, P. F. McMillan and X. Cong, Structure of Calcium Silicate Hydrate (C-S-H): Near-, Mid-, and Far-Infrared Spectroscopy, *J. Am. Ceram. Soc.*, **82(3)**, 742-748 (1999).

Revised : 24.11.2014

Accepted : 26.11.2014